New Journal of Physics

Kinetics of conformational fluctuations in DNA hairpin-loops in crowded fluids

Olivia Stiehl, Kathrin Weidner-Hertrampf and Matthias Weiss[1]

Experimental Physics I, University of Bayreuth, Universitätsstrasse 30, D-95440 Bayreuth, Germany
E-mail: matthias.weiss@uni-bayreuth.de

Abstract. Biochemical reactions in crowded fluids have been predicted to differ strongly from those in aqueous solutions. Both excluded-volume interactions with surrounding macromolecules and crowding-induced subdiffusion have been predicted to stabilize complex formation of reaction partners. Here we show that both facets of crowding strongly alter the stochastic opening and closing of a single-stranded DNA hairpin. Crowding not only slows down the kinetics but also increases the steady-state fraction of closed hairpins significantly. The latter is shown to be enhanced if crowding is associated with subdiffusion. Biochemical reactions in crowded fluids are therefore senssistve to both excluded-volume interactions and changes of the reactants' diffusion characteristics.

Contents

[1] Author to whom any correspondence should be addressed.

IOP Institute of Physics   **Φ** DEUTSCHE PHYSIKALISCHE GESELLSCHAFT

1. Introduction

The cytoplasm of living cells is a highly crowded fluid with a total concentration of macromolecules up to $400\,\mathrm{g\,l^{-1}}$ (Ellis and Minton 2003). Macromolecular crowding has been predicted to enhance protein folding and complex formation due to excluded-volume interactions, and this claim has been supported by simulations and experiments (see Zhou *et al* (2008) for a recent review). Moreover, diffusion in crowded fluids has been shown to be significantly slowed down (Dix and Verkman 2008), and frequently even an anomalous diffusion behavior ('subdiffusion') has been reported (Tolic-Nørrelykke *et al* 2004, Weiss *et al* 2004, Banks and Fradin 2005, Golding and Cox 2006, Tejedor *et al* 2010, Weber *et al* 2010). Subdiffusion is characterized by a nonlinear scaling of the particles' mean square displacement, $\langle r(t)^2 \rangle \sim t^\alpha$ with $\alpha < 1$. Recent experimental data indicate that crowded fluids are viscoelastic on certain scales (Guigas *et al* 2007, Pan *et al* 2009) which forces macromolecules to perform a subdiffusive fractional Brownian motion (FBM) on short and intermediate time scales (Szymanski and Weiss 2009, Ernst *et al* 2012, Weiss 2013). As a consequence, biochemical reactions have been predicted to differ strongly from those in purely viscous solutions (Berry 2002, Hellmann *et al* 2011, 2012). Yet, an experimental support of this claim and a discrimination to mere excluded-volume effects has been lacking so far.

Using fluorescence correlation spectroscopy (FCS) we have quantified the effects of crowding on the opening and closing of a single-stranded DNA hairpin. Similar configurational fluctuations occur in a large class of cellular events, e.g. during gene duplication, transcription and the spontaneous formation of secondary RNA structures (see Alberts *et al* (2002) and references therein for an introduction). We find that altering the viscosity of a purely viscous fluid only reduces the characteristic time scale of the hairpin's conformational fluctuations while the steady-state fraction of closed hairpins is unaffected. In strong contrast, crowded fluids not only exhibit a slowing down of the open/close kinetics but they also show strongly increased steady-state fractions of closed hairpins. The latter phenomenon is even more pronounced when crowding not only provides excluded-volume interactions but when the fluid also has a viscoelastic character, i.e. when the DNA hairpin is subject to subdiffusion.

2. Materials and methods

To probe the conformational fluctuations of a ssDNA hairpin, we followed the approach of Bonnet *et al* (1998), Wallace *et al* (2000, 2001). We have used a $C_3A_2T_{23}G_3$ ssDNA (GenScript Inc., Piscataway, USA) labeled with a rhodamine 5-ROX fluorophore ('control'). In a second $C_3A_2T_{23}G_3$ construct, a BHQ2 quencher was attached to the opposite end of the ssDNA ('beacon'), see also sketch in figure 1. Fluorescence of the beacon in MilliQ water was reduced by 70% at $10\,^{\circ}\mathrm{C}$ in favorable agreement with previous observations that 75–80% of this hairpin construct are in the closed state under these conditions (Wallace *et al* 2001). Opening and closing of the hairpin due to transient binding of the initial five nucleotides (cf. figure 1(a)) therefore gives rise to fluorescence blinking that was monitored by FCS (cf. below). Following Wallace *et al* (2000, 2001) all ssDNA constructs were dissolved in MilliQ water. Under these conditions, the hairpin is melted at room temperature and rapid fluorescence fluctuations due to stochastic opening and closing are expected (Wallace *et al* 2001). We would like to emphasize at this point that the results shown below only exploit the general opening and closing scenario of the hairpin that was shown to be similar at different solvent
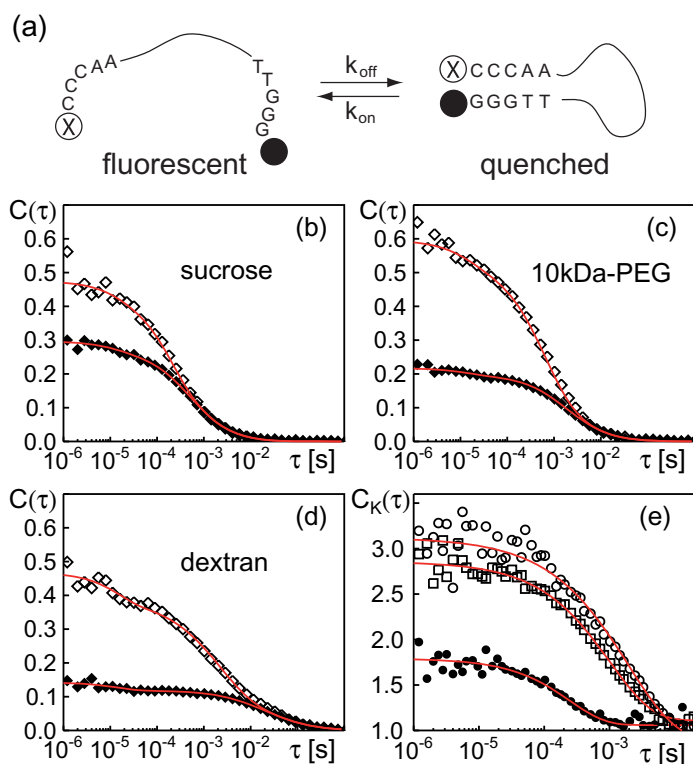
Figure 1. (a) Sketch of the ssDNA hairpin in the open and closed form. Cognate base pairs at the ends are shown explicitly, T bases in the loop are indicated by a full line. The 5-ROX dye and the BHQ2 quencher are shown as open and blackened circles, respectively. (b)–(d) Typical autocorrelation decay $C(\tau)$ of beacon (open symbols) and control ssDNA (full symbols) in fluids with the indicated additives (all 30% by weight). For long times, control and beacon show the same autocorrelation decay due to the ssDNA's center-of-mass diffusion, $C_D(\tau)$. At short times the beacon shows an additional feature due to fluorescence quenching in the closed state. (e) Autocorrelation decay of the beacon's opening/closing kinetics, $C_K(\tau)$, for sucrose (full circles), 10 kDa-polyethylenglycol (PEG) (open squares) and dextran (open circles) solutions (all 30% by weight). Best fits to all curves according to equations (1) and (2), respectively, are shown as red lines.

conditions (Wallace *et al* 2000). To probe the kinetics of conformational ssDNA fluctuations in fluids of different crowdedness, we added varying concentrations of (i) sucrose, (ii) PEG (10 kDa) and (iii) dextran (10 kDa); for comparison, PEG with 200 Da and 4 kDa were used. Dextran and PEG were purchased from Sigma, sucrose from Roth.

FCS was performed at room temperature with a ConfoCor2 (Zeiss, Jena, Germany) using a 40x/1.2NA water immersion objective. For excitation, a 543 nm laser line with an intensity of 700 μW before the objective was used. Fluorescence was detected with a 560 nm long pass filter. For validating our results, a Leica SP5-TCSPC system (Leica Microsystems, Mannheim, Germany and Picoquant, Berlin, Germany) with a 63x/1.2NA water immersion objective (excitation at 561 nm, detection with band pass 607–683 nm) was used. Apart from slightly

different sizes of the confocal volumes, no systematic deviations between both experimental setups were observed. FCS data were evaluated as described earlier (Bonnet *et al* 1998): conformational fluctuations of the ssDNA hairpin were assumed to be statistically independent of the diffusional motion of the entire ssDNA. The total fluorescence autocorrelation function $C(\tau)$ therefore can be written as the product of two correlators $C_D(\tau)$ and $C_K(\tau)$ that describe the fluorescence fluctuations due to diffusion and opening/closing of the hairpin, respectively. For each concentration of sucrose, PEG and dextran, 20–100 FCS measurements of 60 s length were taken for beacon and control, respectively. Data shown below are averages over these individual measurements.

Assuming that opening and closing of the beacon are single-step Poisson processes, the ssDNA's fluorescence fluctuations can be described analogous to a single dye's transition from a fluorescent singlet to a dark triplet state (Bonnet *et al* 1998): $C_K(\tau) = 1 + B \exp(-\tau/\tau_K)$ with $\tau_K = 1/(k_{on} + k_{off})$ being the characteristic time scale of the conformational fluctuations and $B = (1-p)/p$ reporting on the fraction of open ssDNA hairpins, p. However, the somewhat more complex opening/closing of the ssDNA via five base pairs has been shown to lead to a stretched-exponential behavior in the correlator (Wallace *et al* 2000, 2001), i.e.

$$C_K(\tau) = A(1 + B \exp\{-(\tau/\tau_K)^\beta\}) \ . \tag{1}$$

We therefore have evaluated our data with equation (1). Here, the prefactor $A \approx 1$ compensates for unavoidable imprecisions in the division of experimental correlation curves of beacon and control. The exponent $\beta \approx 2/3$ not only accounts for the binding via five cognate bases but also includes the entropic elasticity of the hairpin's poly (T) loop region (Goddard *et al* 2000).

The center-of-mass motion of the ssDNA is well captured by (Weiss *et al* 2004, Szymanski and Weiss 2009)

$$C_D(\tau) = \frac{\mathcal{A}}{(1 + (\tau/\tau_D)^\alpha)\sqrt{1 + q(\tau/\tau_D)^\alpha}} \ , \tag{2}$$

where $\alpha \leqslant 1$ denotes the potential diffusion anomaly and τ_D is the mean residence time of a fluorescent particle in the confocal volume. For normal diffusion ($\alpha = 1$) $\tau_D = r_0^2/(4D)$ with the focal radius r_0 and the particle's diffusion constant D. Elongation of the confocal volume along the optical axis is considered by the parameter $q = 1/25$ that was held fixed throughout the data evaluation process. The prefactor $\mathcal{A}$ in (2) includes the inverse number of fluorescent particles in the confocal volume and may also contain additional photophysics of the non-quenched fluorophore. This photophysics is the same for beacon and control, i.e. $\mathcal{A}_{beacon} = \mathcal{A}_{control}$ if the average number of fluorescent particles in the confocal volume is constant. Hence, in agreement with earlier reports (Bonnet *et al* 1998), the kinetics of the hairpin's conformational fluctuations can be extracted from the ratio of the beacon's and the control's autocorrelation functions.

To complement FCS experiments, we quantified the relative change of the fraction of open ssDNA hairpins in differently crowded fluids by UV absorption. Determining the amount of open DNA structures via hyperchromicity in the spectral range 260–270 nm is a well-established approach (Xodo *et al* 1988). In particular, we monitored the absorption of sucrose, 10 kDa-PEG and dextran solutions (each additive at a concentration of 300 g l^{-1}) with and without the ssDNA construct in the range 200–400 nm with a Jasco V670 spectrophotometer. Absorption spectra were taken in the temperature range 25–60 °C. As a readout for the amount of open

ssDNA hairpins, we quantified the increased absorption at 260 and 270 nm in the presence of the ssDNA as compared to the respective fluid without hairpins.

3. Results and discussion

First, we have monitored the kinetics of our ssDNA constructs (i.e. beacon and control) in MilliQ water containing varying amounts of sucrose. In line with previous results (Bonnet *et al* 1998), both ssDNA constructs showed a diffusion-driven autocorrelation decay (2) for intermediate and large times (figure 1(b)). At short times, the beacon showed an additional contribution $C_K(\tau)$ in the autocorrelation function which reports on the opening and closing of the hairpin (switching between fluorescent and quenched state). Following Bonnet *et al* (1998), the conformational kinetics $C_K(\tau)$ can be extracted by dividing out the control's diffusive autocorrelation decay from the beacon's data, i.e. $C_K(\tau) = C(\tau)/C_D(\tau)$. Indeed, this approach yielded reliable results not only for sucrose solutions but also for PEG and dextran fluids (see representative curves in figure 1). Fitting $C_K(\tau)$ with (1) yielded the characteristic time of the conformational fluctuations, τ_K, and the fraction of open DNA hairpins, p. Consistent with earlier reports (Wallace *et al* 2000, 2001), we found $\beta \approx 2/3$ for all experiments. It is worth noting at this point that β not only summarizes the zipper-like binding event of five cognate bases. It also includes the purely entropic elasticity of the hairpin's poly (T) region in the loop that can be switched to an enthalpic rigidity when using a poly (A) loop (Goddard *et al* 2000). Furthermore, owing to the low concentration of ssDNA in our FCS experiments (about 10 nM) quenching events between two ssDNA copies can be neglected.

Elevated sucrose concentrations increase the fluid's viscosity η but do not lead to subdiffusion of tracer particles (Ernst *et al* 2012). In line with this notion, we observed an increase of the control ssDNA's mean residence time $\tau_D \propto 1/D \propto \eta$ in the focus. In a purely viscous solution, however, opening and closing rates k_{on} and k_{off} can be expected to change similarly with increasing viscosity: the beacon's closing rate can be approximated as a diffusive search of two binding partners separated by the ssDNA length ξ, i.e. $k_{on} \propto D/\xi^2 \propto \eta$. The opening process on the other hand is described by Kramer's escape rate out of a local potential minimum of width ℓ, i.e. $k_{off} \propto D/\ell^2 \propto \eta$. Therefore, τ_K is expected to grow with increasing sucrose concentrations whereas the steady-state fraction of open hairpins, p, should be unaffected. In agreement with this reasoning and in line with previous findings (Wallace *et al* 2001), we observed an increase of τ_K for increasing sucrose concentrations while p remained approximately constant (figure 2).

In strong contrast, crowded fluids not only led to a slowing down of the conformational fluctuations (as quantified via τ_K, figure 2(a)) but they also yielded a significantly lower fraction of open hairpins, p, as the concentration of crowding agents increased (figure 2(b)). Changes of the steady-state fraction of closed ssDNA hairpins were significant for 10 kDa-, 4 kDa-PEG and dextran, whereas 200 Da-PEG (which corresponds in size to sucrose molecules) had no significant effect on p. The observed change in the fraction of closed hairpins in crowded fluids was corroborated by UV absorption measurements on fluids containing 300 g l^{-1} sucrose, 10 kDa-PEG or dextran (see also Methods). In agreement with our FCS experiments, we observed that the UV absorption (reporting on the amount of open hairpins) was reduced by about 16% (PEG) and 70% (dextran) as compared to the sucrose solution. Changes in temperature (from 25 to 60 °C) only lead to minor changes in the absorption levels. Thus, our
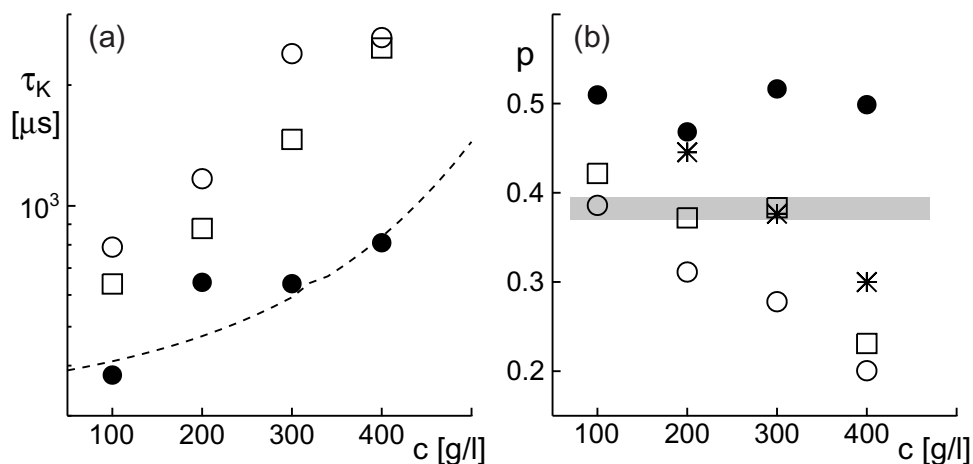
Figure 2. (a) The characteristic time scale of the hairpin's opening and closing, τ_K (shown on a log-scale), grows with increasing concentration of sucrose (full circles), 10 kDa-PEG (open squares) and dextran (open circles). Data for sucrose solutions (viscosity η) are consistent with a previously suggested relation $\tau_K = a_0(a_1 + \eta)^\beta$ (Wallace *et al* 2000) with $a_0 = 220$, $a_1 = 1.2$, $\beta = 0.67$ (dashed line). (b) The fraction of open ssDNA hairpins, p, remains approximately constant for sucrose solutions of different concentrations c (full circles). Also for 200 Da-PEG (gray bar indicating the range between the smallest and largest values), no significant change was observed. In strong contrast, elevated 10 kDa-PEG (open squares), 4 kDa-PEG (asterisks) and dextran (open circles) concentrations induce a strong decrease of p. Hence, the steady-state fraction of closed ssDNA hairpins grows significantly for increasing concentrations of crowders. Error bars are smaller than symbol size in both plots.

FCS data and accompanying UV absorption experiments support the prediction of enhanced complex formation (here: a closed ssDNA hairpin) in crowded fluids (Minton 1981).

Crowding-induced closing of the ssDNA hairpin was strongest when using high concentrations of dextran or 10 kDa-PEG (figure 2(b)). However, a marked difference between these crowders is their structure. While 10 kDa-PEG is a linear polymer with a hydrodynamic radius $R_H \approx 2.8$ nm (Dohmen *et al* 2008), dextran of the same weight is a branched polymer with a considerably smaller hydrodynamic radius $R_H \approx 1.8$ nm (Weiss *et al* 2004). To quantitatively compare the impact of these quite different crowders on the hairpin's open/close kinetics, the volume occupancy rather than the actual concentration should be used. Following this idea, we have defined an apparent (non-normalized) volume occupancy c/c^* via the crossover concentration from dilute to semidilute conditions, $c^* = m/R_H^3$ with m being the molecular mass of the crowder. At c^* crowder molecules start to touch each other. Our choice for c^* is in good agreement with previously reported experimental data on PEG's crossover concentration (Kozer *et al* 2007). As a result, the apparent volume occupancy of 10 kDa-PEG is about 3.8 fold higher than that of dextran.

Comparing the effects of both crowding agents on the basis of the apparent volume occupancy c/c^*, a major difference becomes visible: despite its significantly lower apparent volume occupancy, dextran has about the same impact on the fraction of open ssDNA hairpins
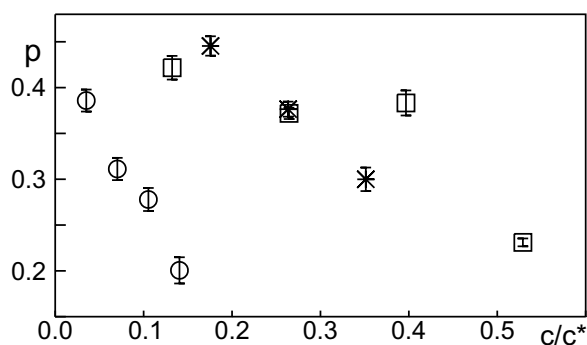
Figure 3. Fraction p of open DNA hairpins as a function of the reduced crowder concentration c/c^* in solutions with 10 kDa-PEG (open squares), 4 kDa-PEG (asterisks), and dextran (open circles). Compared to 10 kDa-PEG, the apparently less densely crowded 10 kDa-dextran solution shows a significantly lower fraction of open ssDNA hairpins. Matching PEG's hydrodynamic radius to that of dextran, i.e. using a 4 kDa-PEG crowder, still a significantly lower fraction of open hairpins is observed for dextran. Error bars are partially smaller than symbol size.

as PEG (figure 3). This result persisted when using a 4 kDa-PEG that matches dextran's hydrodynamic radius. Again, dextran is the more potent crowder as the fraction of open hairpins is significantly lower than for 4 kDa-PEG (figure 3).

To rationalize this phenomenon, it is instructive to inspect the diffusive part of the autocorrelation decay, $C_D(\tau)$, that is best visible in experiments on the control ssDNA (no blinking due to opening/closing of the hairpin). While control ssDNA hairpins showed an almost normal diffusion ($\alpha > 0.9$) in sucrose solutions and PEG-crowded fluids (200 Da, 4 kDa and 10 kDa), a marked subdiffusion ($0.7 \leqslant \alpha \leqslant 0.85$) was observed in dextran-crowded fluids (figure 4). Minor deviations from $\alpha = 1$ for PEG and sucrose are attributed to slight perturbations of the confocal volume (cf Hess and Webb (2002) for discussion). The marked difference in the type of diffusion observed for PEG and dextran compares favorably to previous reports (Weiss *et al* 2004, Banks and Fradin 2005, Kuttner *et al* 2005, Szymanski and Weiss 2009). Indeed, dextran-crowded fluids have been shown to exhibit a viscoelastic behavior on length and time scales below 1 μm and 1 s (Guigas *et al* 2007, Ernst *et al* 2012), and viscoelasticity-induced subdiffusion (i.e. FBM) has been predicted to enhance complex formation (Guigas and Weiss 2008, Hellmann *et al* 2011, 2012). Our data therefore support the idea that the strong effect of dextran crowders on the fraction of open ssDNA hairpins is due to the emergence of crowding-induced subdiffusion.

Neither sucrose nor 200 Da-PEG had a measurable effect on the steady-state fraction of open hairpins, p, whereas the chemically related larger PEGs (4 kDa and 10 kDa) and the polysaccharide dextran induced significant changes. An explanation of the effect solely in terms of enthalpy and the chemical nature of the additive is therefore too simple. Yet, also a pure entropic view (crowders act via excluded-volume interactions) is falling short of explaining our observations as 4 kDa- and 10 kDa-PEG yielded different results from dextran. Most likley, enthalpic contributions in the interaction between the crowders are responsible for the emergence of subdiffusion and the enhanced fraction of closed ssDNA
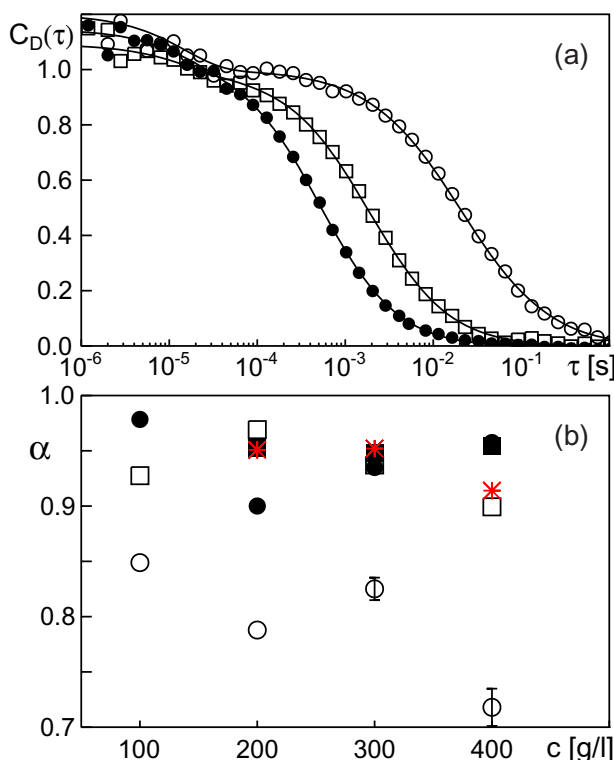
Figure 4. (a) Representative autocorrelation curves of control ssDNA in sucrose (filled circles), 10 kDa-PEG (open squares) and dextran (open circles) solutions (30% by weight). Due to the missing quencher, $C(\tau) = C_{\mathrm{D}}(\tau)$ (full lines are best fits with (2)). (b) Diffusion anomaly α for different crowder concentrations as extracted from (2). Sucrose and 200 Da-PEG (filled circles and squares) as well as 4 kDa-PEG and 10 kDa-PEG solutions (red asterisks and open squares) are consistent with normal diffusion, $\alpha = 1$. In contrast, dextran solutions show a concentration-dependent anomaly in the range $0.7 \leqslant \alpha \leqslant 0.85$ (open circles) that is consistent with earlier observations (Weiss *et al* 2004, Banks and Fradin 2005, Szymanski and Weiss 2009). Only error bars that are larger than symbol size are shown.

hairpins. Macromolecular crowding therefore is more than mere excluded-volume interactions: crowding-induced viscoelastic characteristics of the fluid and the associated emergence of subdiffusion are an additional facette that can drastically alter biochemical reactions.

Acknowledgments

References

Alberts B, Johnson A, Lewis J, Raff M, Roberts K and Walter P 2002 *Molecular Biology of the Cell* 4 edn (New York: Garland Science)

Banks D and Fradin C 2005 *Biophys. J.* **89** 2960–71

Berry H 2002 *Biophys. J.* **83** 1891–901

Bonnet G, Krichevsky O and Libchaber A 1998 *Proc. Natl Acad. Sci. USA* **95** 8602–6

Dix J A and Verkman A S 2008 *Ann. Rev. Biophys.* **37** 247

Dohmen M P J, Pereira A M, Timmer J M K, Benes N E and Keurentjes J T F 2008 *J. Chem. Eng. Data* **53** 63–5

Ellis J R and Minton A P 2003 *Nature* **425** 27–8

Ernst D, Hellmann M, Kohler J and Weiss M 2012 *Soft Matter* **8** 4886

Goddard N, Bonnet G, Krichevsky O and Libchaber A 2000 *Phys. Rev. Lett.* **85** 2400–3

Golding I and Cox E C 2006 *Phys. Rev. Lett.* **96** 098102

Guigas G, Kalla C and Weiss M 2007 *Biophys. J.* **93** 316

Guigas G and Weiss M 2008 *Biophys. J.* **94** 90–4

Hellmann M, Heermann D and Weiss M 2011 *Europhys. Lett.* **94** 18002

Hellmann M, Heermann D and Weiss M 2012 *Europhys. Lett.* **97** 58004

Hess S T and Webb W W 2002 *Biophys. J.* **83** 2300–17

Kozer N, Kuttner Y Y, Haran G and Schreiber G 2007 *Biophys. J.* **92** 2139–49

Kuttner Y Y, Kozer N, Segal E, Schreiber G and Haran G 2005 *JACS* **127** 15138–44

Minton A P 1981 *Biopolymers* **20** 2093–120

Pan W, Filobelo L, Pham N D Q, Galkin O, Uzunova V V and Vekilov P G 2009 *Phys. Rev. Lett.* **102** 058101

Szymanski J and Weiss M 2009 *Phys. Rev. Lett.* **103** 038102

Tejedor V, Bénichou O, Voituriez R, Jungmann R, Simmel F, Selhuber-Unkel C, Oddershede L B and Metzler R 2010 *Biophys. J.* **98** 1364–72

Tolic-Nørrelykke I, Munteanu E, Thon G, Oddershede L and Berg-Sørensen K 2004 *Phys. Rev. Lett.* **93** 078102

Wallace M I, Ying L, Balasubramanian S and Klenerman D 2000 *J. Phys. Chem.* B **104** 11551–5

Wallace M I, Ying L, Balasubramanian S and Klenerman D 2001 *Proc. Natl Acad. Sci. USA* **98** 5584–9

Weber S C, Spakowitz A J and Theriot J A 2010 *Phys. Rev. Lett.* **104** 238102

Weiss M 2013 *Phys. Rev.* E **88** 010101

Weiss M, Elsner M, Kartberg F and Nilsson T 2004 *Biophys. J.* **87** 3518–24

Xodo L, Manzini G, Quadrifoglio F, van der Marel G and van Boom J 1988 *Biochemistry* **27** 6327–31

Zhou H X, Rivas G and Minton A P 2008 *Ann. Rev. Biophys.* **37** 375–97